Int J Pharm Bio Sci 2012 Oct; 3(4): (B) 102 - 120

Research Article **Bioinformatics**

International Journal of Pharma and Bio Sciences **ISSN 0975-6299**

MOLECULAR MODELING OF INOSINE 5'- MONOPHOSPHATE DEHYDROGENASE-II (HUMAN) STRUCTURE USING MD-SIMULATION METHOD

DEEPAK K. MISHRA, BISHNU P. MUKHOPADHYAY* AND HRIDOY R. BAIRAGYA

Department of Chemistry, National Institute of Technology-Durgapur, West Bengal, India

ABSTRACT

Inosine 5'- monophosphate dehydrogenase of human (hIMPDH) is involved in GMP nucleotide biosynthesis pathway. Type II isoform is found in the human CML cells. Recently the enzyme is actively targeted for the development of anticancer and antleukemic agent. Till todate, a few low resolution 3D X-ray structures (contain 75% residues) of hIMPDH-II are available in PDB. For making a better three-dimensional model structure (with full sequence 514 residues) of hIMPDH-II molecular modeling methods have been attempted. Addition of 25% residues, energy minimization and 50 ns MD-simulation are successively followed for modeling of protein. The quality of final model structure has been validated by different modeling tools. The internal potential energy, stability free energy, solvation free energy, 3D profile quality index and Z-score values have clearly indicated the goodness of final refined model structure compared to hIMPDH-II X-ray structure. The model provides a detail stereochemical insight on the secondary structure and folding pattern of protein. The model may be used for docking studies (with different ligands) and insilico inhibitor design.

KEYWORDS: hIMPDH-II, Molecular Modeling, MD-simulation, Drug target and CML

B. P. MUKHOPADHYAY
Department of Chemistry, National Institute of Technology-Durgapur, West Bengal, India

Corresponding author

INTRODUCTION

Inosine 5'- monophosphate dehydrogenase (IMPDH) is involved in the GMP (Guanosine monophosphate) nucleotide biosynthesis pathway[1]. Type II isoform of enzyme is selectively up-regulated in neoplastic and replicating cells, and also found in proliferating chronic myelogenous leukemia (CML) cancer cells of human. In recent time, hIMPDH–II is actively targeted for the development of anticancer and antiviral agent[2,3]. Attempts have been made to elucidate the binding mechanism of IMP and NAD^+ or their structural analogs/inhibitors to IMPDH at molecular level. Recently, some research work on conserved water molecular dynamics in hIMPDH have been investigated, which are used for inhibitor design using water mimic inhibitor design protocol.[4-6] However, till now no detail information is available on the structural and dynamical features of hIMPDH enzyme[4-6]. In mammalian species, the IMPDH has two isoforms (I and II) with 84 % amino acid identity. The 1B3O, 1NF7 and 1NFB[7-9] PDB-structures of hIMPDH-II are available as inhibitor bound conformation, though detail structural information of later two structures are lacking in PDB. The only published work of 1B3O (which diffracts upto 2.9 Å resolution) is also contained disorder at several sites and poorly defined electron density at ∽25% of the total 514 residues of protein[10]. In X-ray crystal structure of 1B3O, the polypeptide sequences from 1-9, 129–139, 159–177, 400–448 and 499–514 (total 104 number of residues) are missing and cannot be predicted experimentally due to very weak and unclear electron densities in these regions. So, for making a better three-dimensional model structure of hIMPDH-II, these missing fragments have been incorporated and reconstructed by molecular modeling[11]. The quality of final modeled structure has been validated by different modeling tools and also compared with the 1B3O X-ray structure. The well-refined simulated 1B3O structure with complete amino acids sequence (514 residues) would always be a better structural model for hIMPDH–II and useful for getting an insight to the dynamical conformation of unliganded structure. The modeled structure may be used in docking of IMP, NAD^+ or their structural analogs and insilico inhibitor design. Moreover, MD-simulation results may provide some dynamical aspects, stereochemical insight on secondary structures and folding of the protein which is inaccessible in the X-ray structure.

MATERIALS AND METHODS

The crystallographic structure of 1B3O (hIMPDH type II) was obtained from the Protein Data Bank[12], where two molecules (A and B) were present in the asymmetric unit. From the PDB structure, B molecule was selected (excluding ligands and water molecules) using Swiss PDB Viewer program[13,14]. The missing 104 residues (res. id.1-9, 129-139, 159-177, 400-448 and 499-514) were obtained from Protein Data Bank and successively incorporated in the missing gaps. Preliminary structural information of different hIMPDH- II are given in Table 1. The 1B3O structure was modeled by MD (Molecular Dynamics) simulation methods.

Table 1
Preliminary Structural Information on IMPDH II (Human) X-ray crystal structures

	1B3O	1NFB	1NF7
Resolution (Å)/ R- Value	2.90/.244	2.90/0.229	2.65/0.238
No. of Protein chain and water molecules in asymmetric unit.	2 (A, B)/ 11, 20	2 (A, B)/ 43, 44	2 (A, B)/ 46, 46
Domains	($*I_N$,$*C_1$,$*C_2$,$*I_C$)	($*I_N$,$*C_1$,$*C_2$,$*I_C$)	($*I_N$,$*C_1$,$*C_2$,$*I_C$)
Total no. of missing residues/ (residue No.)	104/ (1 -9 , 129 – 139 , 159 – 177 , 400 – 448 , 499 – 514)	117/ (1 – 9 , 124 – 140 , 153 – 187 , 224 – 229 , 415 – 448 , 499 – 514)	60/ (1-9 , 125 – 155 , 167 – 169 , 226 , 412 – 436)
α Helix/ β Sheet/ Coil	12/ 20/ 33	11/ 16/ 28	14/ 19/ 34

I_N and I_C indicates N and C-terminal domains (residue no: 28-111 and 233-504).
C_1 and C_2 indicates the CBS 1 and CBS 2 domains (residue no: 112-171 and 172-232).

Inclusion of missing residues in the X-ray structure

The amino acid sequences/ residues were covalently added in the respective five gaps (starting from N- to C- terminal) within the X-ray structure of 1B30 using Swiss PDB Viewer program. Each residue was refined after incorporating in the protein structure, by implementing GROMOS 96 force field[15] in the Swiss PDB Viewer program. Energy minimization was performed (500 steps of steepest descent followed by 1000 steps of conjugate gradient) without assigning any constraint. The added residue was allowed to move freely until it could adopt stereochemically compatible conformation with minimum energy. Then the five missing fragments (containing the respective amino acid residues) were energy minimized (keeping other residues fixed) till the ΔE value reached to ∽ .001 kJ/mol for avoiding steric hindrance. The energy minimized 1B3O structure(containing the entire sequence) was again energy minimized for 500 steps of steepest descent followed by 1000 cycles of conjugate gradient using GROMOS 96 force field in Swiss PDB Viewer program with a 10 Å cutoff distance[16] for the non-bonded interaction and distance dependent dielectric constant. Again the X-ray structure of 1B3O was modeled using the program MODELLER[41] to built the model of structural segment of lacking residues (104) in the protein. Then the IMP and NAD^+ were fitted within their corresponding pockets in the IMPDH using the program Swiss PDB Viewer.

Solvation of energy minimized structure

Generally solvent exposed side chains, which interact with water molecule in protein crystal, are unable to find their enthalpic counterparts in *vacuo,* and readily establish interactions within protein that globally distort the structure. These problems can be avoided by simulating the protein in water, with periodic boundary conditions[17] which eliminate the artifacts arising from the system----vacuum interface. Interaction between water and protein form an essential part of the balance of enthalpic and entropic effects which stabilize the three dimensional structure of a protein[18]. Again, concerning the role of water molecules in stabilizing of 3D structure of enzyme[19-21], we have solvated the energy minimized structure (unliganded and liganded) before simulation. To avoid unnecessary inclusion of excess

number of water molecules, the energy minimized structure was solvated by program CHASA (Conditional Hydrophobic Accessible Surface Area)[22]. The TIP3P model of water molecules was used to immerse the structure taking probe radius of 1.4Å for solvation.

Refinement of model structure by Molecular Dynamics (MD) simulation

For obtaining the better refined 3D structure of 1B3O, extensive 50 ns MD simulation was carried out on the solvated energy minimized model structure of protein. Before simulation, Protein Structure File (PSF) of solvated energy minimized structure was generated by Automatic PSF Generation Plugin –v 1.0. assign the CHARMM 27 force field[23,24] within the Visual Molecular Dynamics (VMD) v. 1.8.6 program[25]. Initially the structure was energy minimized (for 100 cycles using CHARMM 27 force field to eliminate the initial contacts which would destabilize the system) and then simulated using Auto-Interactive Molecular Dynamics[26] connected between the visualization program VMD v. 1.8.6 and the Molecular Dynamics program Nanoscale Moloecular Dynamics v. 2.7.[27,28]. The Molecular Dynamics simulation was implied on the entire system with periodic boundary condition where all the residues and water molecules were allowed to move freely. The simulation was performed on Super Micro system using configuration of Central Processing Unit (CPU) and Graphical Processing Unit conjugation (GPU) (8 CPU and 4 GPU). The dynamics was performed up to 50 ns without applying any constrain (with time step 2 fs) at 300 K temperature using Langevin dynamics[29]. The solvated structure was converged within 20 ns, however, further simulation was continued up to 50 ns for obtaining a well converged and refined structure[30]. The fluctuations in potential energy, kinetic energy and total energy were monitored during the entire simulation period. The plot of potential energy against time at constant temperature (300K) revealed that the equilibrium was attained when the average potential energy and kinetic energy were constant and simulations were seems to be adequately converged within 20 ns[31]. At equilibrium state, negligible variation of RMSD (Fig. 1), stability free energy and conformational stability energy were observed (Fig. 2). Again the solvated liganded hIMPDH structures (containing IMP and NAD^+) were taken for simulation studies. Parameterization of the ligands (IMP and NAD^+) were done by SwissParam program[42]. The topology and parameter files of each ligand were compatible with CHARMM22 force field for MD-simulation. The simulation protocols, parameters and configuration files of the structure were followed as mentioned earlier and the simulation was performed upto 50ns.

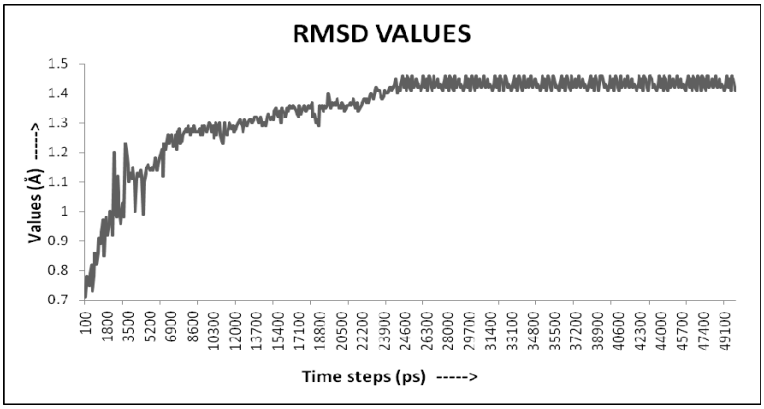

Figure 1
RMSD backbone of the MD simulated 1B3O structure at different snapshots.

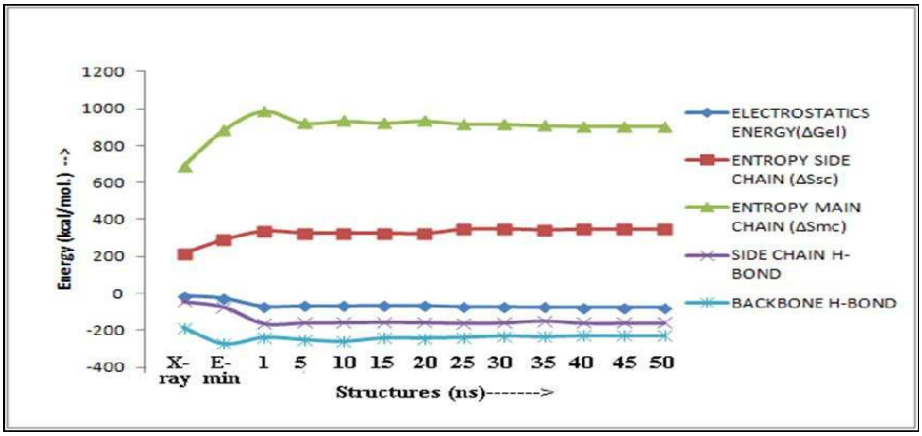

Figure 2
Stability free energy (∆G_{el}, ∆S_{sc}, ∆S_{mc}, side chain and backbone H-bond) of the X-ray, E-Min and MD simulated 1B3O structures at different snapshots.

Model evaluation

The X-ray, E-min (energy minimized) and MD-simulated structures (liganded and unliganded 50ns structures) were critically analyzed by Structural Analysis and Verification Server (SAVS) and also by employing other computational tools and software to find the quality of reconstructed model structure. Several parameters were calculated in order to assess the stereochemical quality of protein model by PROCHECK program[32]. The parameters such as main chain bond lengths and bond angles, peptide bond angle distribution, Cα tetrahedral distortion, phi/psi Ramachandran plot distribution, main-chain hydrogen-bond energies, and overall G-factor were calculated and compared with the expected values derived from a database of high-resolution protein structure. The non-bonded interaction energy was thoroughly checked and calibrated using program ERRAT[33]. The secondary structure (helix, beta strand, coil and turn), accessible surface area (ASA), volume, packing fraction, folding free energies, residues with hydrogen bonding interaction were calculated using VADAR (Volume Area Dihedral Angle Reporter) v. 1.8[34]. MolProbity web server was also used for calculating and visualizing the bad contacts, atomic overlaps, and Cβ positions deviations[35]. ProsaII was also used to evaluate the pseudo energy of pair-wise interaction from the spatial separation of residues[36,37]. The final 3D modeled structure of 1B3O was verified by program Verify3D[38].

Calculation of stability free energy, internal potential energy and solvation free energy

Stability free energy of the X-ray, energy minimized and MD-simulated 1B3O structures were calculated at different time steps using program FOLDX (v. 3.0.)[39]. The temperature, ionic strength, pH and VDW (parameters of the FOLDX) were assigned as 300K, 0.05 (M), 7.0 and 2 respectively.

The internal potential energy of X-ray, E-min and MD simulated structures (at the 1, 5, 10, 15, 20, 25, 30, 35, 40, 45 and 50 ns) were calculated using NAMD energy plugin Version 1.4 in VMD program (Fig. 3). The CHARMM 27 force field was used to calculate the energy.

The solvation free energy (ΔG_{sol}) of X-ray, E-min and MD simulated structures were calculated using CHASA program (Fig. 4)

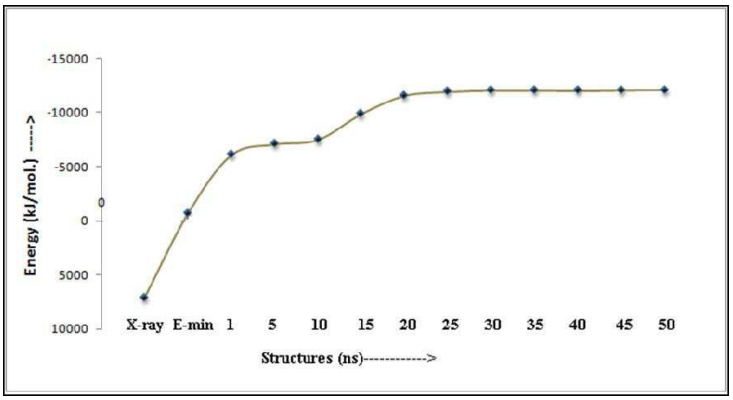

Figure 3
Internal potential energy (kcal/mol) of the X-ray, E-Min and MD simulated 1B3O structures at different snapshots.

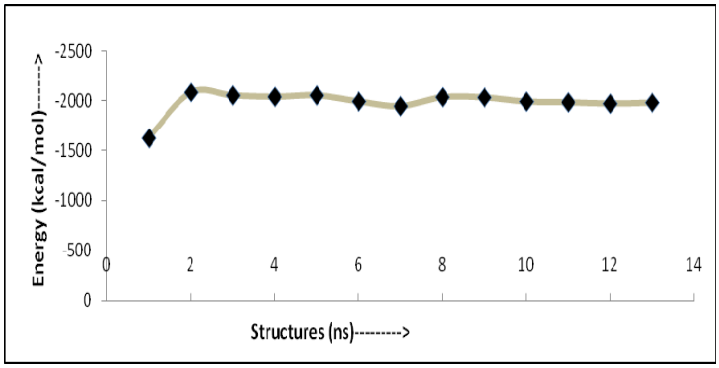

Figure 4
Solvation free energy (ΔG_{Sol} in kcal/mol) of the X-ray, E-Min and MD simulated 1B3O structures at different snapshots.

RESULTS AND DISCUSSIONS

Analysis of X-ray crystal structure of 1B3O

The secondary structural features of 1B3O, 1NFB and 1NF7 X-ray structures are analyzed by SPDBV version 4.0 (Table 2). The stereochemical quality (PROCHECK, VADAR), non-bonded interaction (ERRAT), compatibility of 3D atomic model with 1D amino acid sequence (Verify3D) and other global quality scores (Z-score) of the 1B3O PDB-structure are thoroughly checked before the modeling of structure. However, those values are not sufficiently enough for being a good-quality structure. The Overall Quality Factor of the 1B3O crystal structure is 80.366 (determined by ERRAT program embedded in Structural Analysis and Verification Server (SAVS). Again, 80% of 410 residues (present in the X-ray structure) of protein falls below the 95% rejection limit of the calculated error value. Possibly, 104 number of missing residues in X-ray structure may influence the structural variation. Stereochemical quality including the main-chain bond-length, main-chain bond angle and Ramachandran Plot of the structure are checked by PROCHECK. In that structure 99.8% bond-length is within the limit, however error is observed in bond angles. Remaining 0.2% error in the main-chain bond length included the amino-acid residues Thr10, Ile144, Arg182, Val186, Lys229 and Val336.

Few other residues e.g., Asp16, Thr74, Asn94, Glu111, Gly113, Ser152, Lys181, Lys228 and Lys229 having average error (~12^0) in bond angle. The accessible surface area (ASA) 19646.40 $Å^2$ seems higher than the expected value 18399.78 $Å^2$. The packing volume is 53681.3 $Å^3$, however the expected value 67913.3 $Å^3$ seems to be higher for the total 410 residues (Table 3A). Verify3D shows that 96.35% of the amino acid residues of X-ray structure had an averaged 3D-1D score greater than 0.2, however the structure had many number of missing (104) residues which were not considered for scoring calculation (Table 3B). The calculation of clash score (number of bad overlaps per 1000 atoms) is done by MolProbity. The clash score of 1B3O X-ray structure is 61.09, which seems to be five times greater than 50 ns MD-simulated structure.

Table 2

Secondary structures of 1B3O in the X-ray , E-min and MD-simulated structures.

		X-ray structure with incomplete sequence.			Modeled structure (with full sequence)		
Secondary structure		α Helix	β Sheet	Coil	α Helix	β Sheet	Coil
X-ray		12	20	33	-----	-----	----
E-min		-----	-----	-----	3-8, 402-405, 432-447, 499-513	159-160, 411-414	1-2, 129-139, 161-177, 400-401, 406-410, 415-431, 514
MD-simulated (solvated) structure (ns)	1	-----	-----	-----	3-6, 417-421	407-413, 443- 448	1-2, 7-9, 129-139, 159-177, 400-406, 414-416, 422-442, 499-514
	10	-----	-----	-----	417-420	407-413, 443-448	1-9,129-139,159-177,400-406,414-416,421-442, 499-514
	20	-----	-----	-----	418-419, 502-506	401-403, 406-413, 443-448	1-9,129-139,159-177,400,404-405, 414-417,420-442, 499-501,507-514
	30	-----	-----	-----	3-6, 76-84, 97-108, 149-152, 197-203, 256-266, 281-284, 288-292, 307-315, 343-357, 375-377, 418-420, 458-462, 469-470, 499-503	34-38, 53-55, 59-61, 64-66, 89-91, 124-126, 172-174, 209-213, 217-222, 247-250, 270-274, 298-302, 321-323, 321-323360-365, 383-386, 383-386, 401-403, 406-408, 411-413, 443-445, 489-493	7-33, 39-52, 56-58, 67-75, 85-88, 92-96, 109-123, 127-148, 153-171, 175-196, 204-208, 214-216, 223-246, 251-255, 267-269, 275-280, 285-287, 293-297, 303-306, 316-320, 324-342, 366-374, 378-382, 387-400, 404-405, 409-410, 414-417, 421-442, 446-457, 463-468, 471-488, 494-498, 504-514

	40	-----	-----	-----	76-85, 97-108, 197-204, 256-266, 281-284, 288-290, 307-316, 343-355, 374-378, 458-462, 499-503	34-38, 53-55, 59-61, 64-66, 89-91, 124-126, 172-174, 209-213, 217-222, 237-239, 243-245, 247-250, 269-274, 298-302, 320-323, 362-365, 383-386,	1-33, 39-52, 56-58, 67-75, 92-96, 109-123, 127-151, 153-171, 175-195, 205-208, 214-216, 223-236, 240-242, 251-255, 275-280, 285-287, 291-297, 303-306, 317-319, 324-342, 356-361-366-
						407-413, 443-449, 489-493	373, 379-382, 388-390, 392-406, 414-417, 420-442, 450-457, 463-488, 494-498, 504-514
	50	-----	-----	-----	20-25, 76-84, 97-108, 148-152, 197-204, 256-266, 281-284, 288-290, 307-316, 343-356, 375-378, 387-390, 418-419, 458-464, 499-503	34-38, 53-55, 59-61, 64-66, 89-91, 124-126, 172-174, 209-213, 217-222, 237-239, 243-245, 247-250, 271-274, 298-300, 321-323, 360-365, 383-386, 407-414, 442-449, 489-493	1-19, 26-33, 39-52, 56-58, 67-75, 85-88, 92-96, 109-123, 127-147, 153-171, 175-196, 205-208, 214-216, 223-236, 240-242, 251-255, 267-270, 275-280, 285-287, 291-297, 301-306, 317-320, 324-342, 357-359, 366-374, 379-374, 391-406, 415-417, 420-441, 450-457, 465-488, 494-498, 504-514

Table 3A

(Stereochemical Parameters of the X-ray and MD simulated structure of 1B3O (with full

1B3O (B-chain) PDB structure	Total ASA ($Å^2$)	Total Volume (Packing) ($Å^3$)	Residue with H-bonds	Residue in phi/psi core	Residue in omega core	Free energy of folding (K.cal/mole)	Residue 95% buried	Helix	Beta	Coil	Turn
X-ray	19646.4	53681.3	297 (71%)	317 (76%)	414 (100%)	-367.89	122	30%	28%	40%	18%
E-min	24726.7	73583.3	387 (75%)	403 (78%)	413 (80%)	-369.31	145	33%	23%	42%	19%
Simulated structures with solvent (ns) 1	19912.1	71428.4	337 (65%)	363 (70%)	325 (63%)	-326.10	193	19%	23%	57%	20%
5	19704.1	70987.5	328 (63%)	366 (71%)	334 (64%)	-326.89	200	21%	21%	56%	17%
10	19757	71274.2	340 (66%)	367 (71%)	337 (65%)	-330.60	199	20%	23%	55%	19%
15	19626.9	71437.5	347 (67%)	377 (73%)	337 (65%)	-334.50	204	21%	22%	55%	17%
20	19885.5	72404.3	332 (64%)	358 (69%)	323 (62%)	-330.77	210	22%	23%	54%	13%
25	19143.8	71495.6	341 (66%)	403 (78%)	327 (63%)	-385.42	210	21%	23%	55%	21%
30	19715.3	70407.7	330 (64%)	408 (79%)	337 (65%)	-370.09	192	19%	23%	56%	36%
35	19857.8	71649.9	328 (63%)	413 (80%)	313 (61%)	-369.14	187	19%	22%	58%	7%
40	19426.8	70332.7	335 (65%)	429 (83%)	343 ()66%	-368.07	186	20%	22%	56%	7%
45	19879.6	17616.6	325 (63%)	413 (80%)	334 (65%)	-366.64	192	18%	22%	59%	8%
50	19664.3	70401.6	329 (64%)	424 (82%)	332 (64%)	-369.03	190	21%	23%	55%	10%

Table 3B
3D-1D score and the overall Model Quality of the X-ray and simulated structure of 1B3O.

1B3O PDB Structure (B-chain)	Verify3D (% of the residues had an averaged 3D-1D score > 0.2)	ProSA Overall Model Quality (Z-Score)
1B3O (X-ray)	96.35%	-6.85
Emin	80.00%	-6.24
simulated (with solvent) ns 1	76.50%	-6.57
5	78.64%	
10	74.76%	-7.15
15	76.89%	-6.65
20	82.33%	-6.35
25	99.3%	-7.10
30	98.67%	-7.00
35	99.3%	-6.90
40	98.67%	-6.95
45	99.03%	-6.70
50	99.33%	-6.71

Analysis of 50 ns simulated model structure
After incorporating the 104 number of missing residues in the native 1B3O protein, the structure was energy minimized and then 50 ns MD-simulation was performed. Some changes in the secondary structures are observed in energy minimized and MD-simulated structures at different time. Overall quality factor of simulated/refined model structure (calculated by ERRAT program) is 96.03. The model structure seems to be better and more refined compared to X-ray structure. Stereochemical quality of the 50 ns simulated modeled structure (checked by PROCHEK) seems to be improved compare to initial structure. Most of the stereochemical parameters are in consistent with high-resolution (2 Å) structures of the database (PROCHECK). Moreover, 100% bond-length of the protein structure lies within the limit including those residues (Thr10, Ile144, Arg182, Val186, Lys229, and Val336) which were found to be distorted in X-ray structure. In the final MD-simulated structure, the bond-angle does not contain any off graph containing the outlier as it was observed at several residues in the X-ray structure. In 50 ns simulated structure 98.5% residues are lying within the allowed region of Ramachandran plot, including Thr116 which was distorted in PDB structure. During simulation, the missing residues (Ser425, Asp172, Lys167, Lys410 and the active site Tyr411) which were in the disallowed region (in E-min structure) have also been moved in the favoured zone. Other local and global quality parameters such as accessible surface area (ASA), packing, number of residues in phi/psi and omega core of MD-simulated structures at different time interval (snapshots) are analyzed using different computational programs. The results reveal that the model structure is reasonably more better than 1B3O X-ray structure. The

ASA value 19664.3 $Å^2$ and total volume (packing) 70401.6 $Å^3$of the modeled structure (containing 514 amino acid residues) are also improved. The Z-score value, -6.71 (obtained from PROSA web-services) is in the range of native protein structures having same number of amino acid residues. Verify3D determines the compatibility of atomic model (3D) with the amino acid sequence (1D) by assigning a structural class based on its location and environment, and compares the results to good structures. Verify3D scores have also indicated the goodness of 50 ns model 1B3O structure, where 99.33% of amino acid residues have an averaged 3D-1D score greater than 0.04. However, only few (0.77%) residues (Glu433, Ala434, Asp435 and Lys438) have shown some negative score ranging from -0.01 to -0.08. The simulated structures (1-50ns) of liganded and unliganded form were verified and included in Table4.

Table 4
The parameters (for model verification) of liganded and unliganded MD-simulated structures.

	MD-simulated structures (ns)	Verify3D	Errat	Prosa II
Unliganded	1	76.50%	77.84	-6.57
	10	74.76%	80.79	-7.15
	20	82.33%	95.02	-6.35
	30	98.67%	89.00	-7.00
	40	98.67%	88.66	-6.95
	50	99.33%	96.03	-6.71
Liganded	1	99.42%	93.81	-8.15
	10	100%	89.64	-7.83
	20	99.42%	90.41	-7.04
	30	99.42%	85.62	-6.70
	40	99.42%	90.60	-7.07
	50	99.33%	88.93	-7.09

Packing / Stereochemical quality of 1B3O model structure

Packing/Stereochemical quality[40] were assessed by considering certain parameters such as torsion angle, omega angle and van der Waals parameter. It will provide scores ranging from 0 (worst) to 3 (best) for each of the parameter with total score 9 for each amino acid residue. The Packing Quality Index of many residues have been improved in the modeled structure. Stereochemical Quality of the amino acid residues Gly77, Gly113, Thr116, Asp117, Pro123, Asp129, Ser159, Ala223, Thr252, Ile332, Ala338, Gly365, Ala374, Gly387, and Val499 are substantially improved after simulation and 80% residues in the modeled structure did not indicate any possible problem. However, ~7% of the total residues having problem particularly when the van der Waals parameter was considered.

Solvation energy, internal potential energy and stability free-energy of the MD-simulated structure

The backbone H-bond energy, sidechain H-bond energy, van der Waals (ΔG_{vdw}), electrostatic (ΔG_{el}), solvation polar (ΔG_{solvP}), solvation hydrophobic (ΔG_{solvH}), entropy side chain (ΔS_{sc}), entropy main chain (ΔS_{mc}) are calculated for the simulated 1B3O structure at different snapshots. Solvation energy of 50 ns simulated structure (-2037.57 kcal/mol), shows a higher propensity of solvation compare to initial X-ray structure (-197.33 kcal/mol). Internal potential energy (-12112.1 kcal/mol) has indicated the better stabilization of simulated structure compared to X-ray structure (7074 kcal/mol), RMSD of Cα atoms in the final modeled structure (compared to native X-ray structure) the found to be within 1.30-1.48 Å. The RMSD (at different time interval) for the backbone atoms, sidechain atoms, and all atoms are included in Table 3C.

Table 3C

RMSD fluctuation (Å) of energy minimized and MD-simulated 1B3O structure from the X-ray structure.

Atoms	E-min (structure)	MD-simulated (solvated) structure (ns)										
		1	5	10	15	20	25	30	35	40	45	50
Cα carbon	0.09	1.44	1.45	1.48	1.34	1.30	1.37	1.33	1.31	1.37	1.31	1.23
Backbone	0.36	1.45	1.45	1.54	1.38	1.40	1.44	1.40	1.37	1.44	1.37	1.30
Side chain	0.36	1.45	1.45	1.54	1.38	1.40	1.44	1.40	1.37	1.44	1.37	1.30
All atoms	0.36	1.45	1.45	1.54	1.38	1.40	1.44	1.40	1.37	1.44	1.37	1.30

Comparative study of X-ray and MD-simulated structure

Comparative results of different parameters of the X-ray, E-min and final MD-simulated structures are shown in Fig. 5. Structures at different snapshots are also shown in Fig. 6 which may help for understanding the variation or refinement of dynamical structures at different time. The unliganded initial and its final simulated structure indicate the change of structural motif during dynamics which is shown in Fig.7. Moreover, the initial structure of ligand bound conformation and its simulated form could also reveal the variation of secondary topology of the protein which is shown in Fig. 8. In the simulated structures of unliganded and liganded conformation, the numbers of helix, sheet and coil are included in Table 5. The internal potential and folding free energy of X-ray structure are 7074.0 and -366.26 kcal/mol, whereas for the simulated conformation (with full sequence) the values are -12112.10 and -369.03 kcal/mol respectively. Moreover, the stability free energy especially for the electrostatic energy (ΔG_{el}), H-bond energy of backbone and side chain of the X-ray structure are -13.93,-41.42 and -185.06 kcal/mol, but the values are -76.56, -229.16 and -159.04 kcal/mol in the final simulated structure. In addition, solvation free energy (ΔG_{sol}) of X-ray structure -1618.93 has also been decreased to -2037.00 kcal/mol for final simulated form**.** The 96.03% residues of simulated structure are lying below the rejected region of non-bonding interaction (calculated by ERRAT program), however 82.36% residues are observed for X-ray structure. The Z-score value -6.71 of MD-simulated structure seems comparable to -6.85 of X-ray structure (having incomplete sequence). So, theoretical parameters of the structure e.g., internal potential energy, stability free energy, solvation free energy, 3D profile quality index and Z-score values have clearly indicated the goodness of final 50 ns simulated model hIMPDH-II structure compare to X-ray structure(Fig. 5.)

.

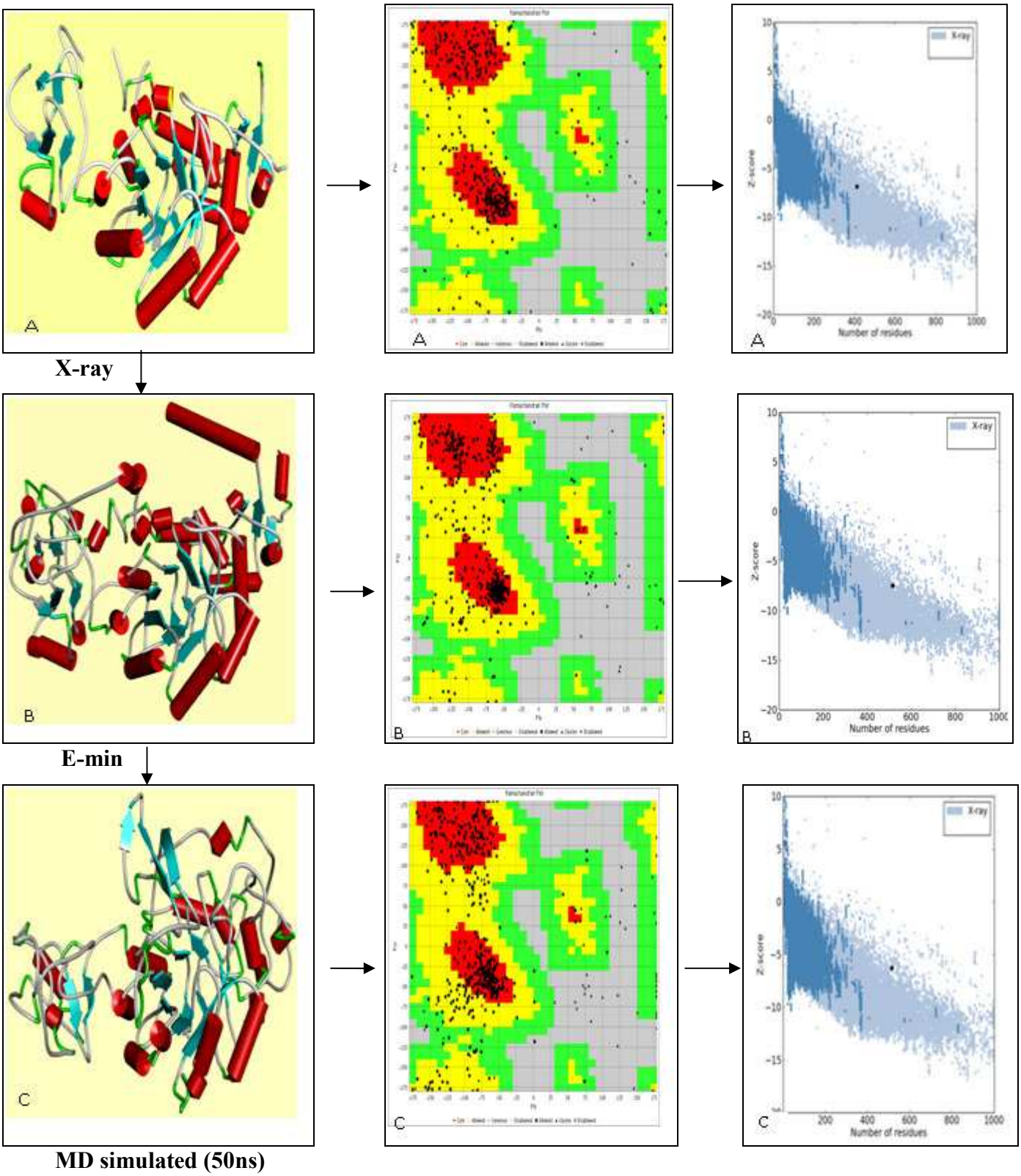

Figure 5
Ramchandran Plot and Z-score of X-ray, E-Min and MD-Simulated structures.

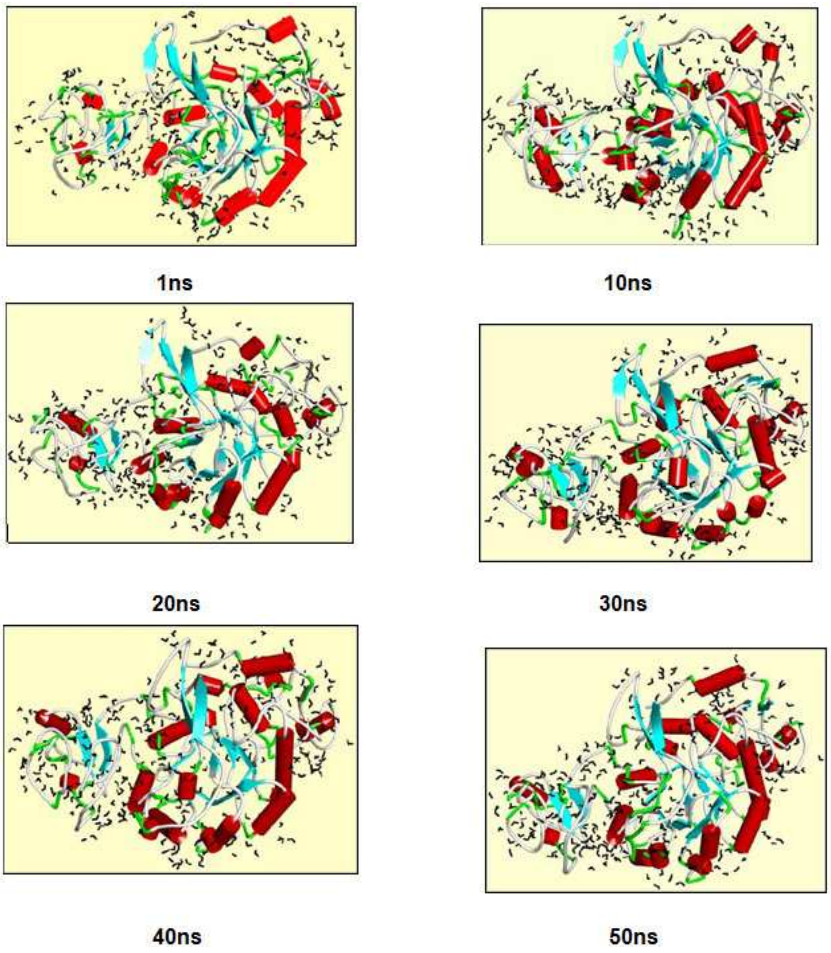

Figure 6
Conformational transition of 1B3O MD-Simulated structure from initial to final modeled Structure.

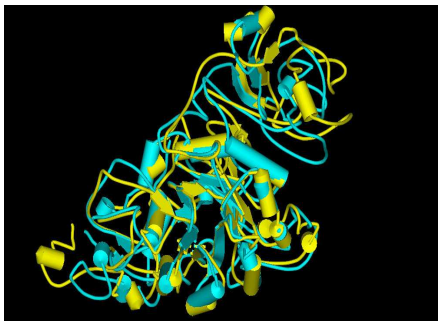

Figure 7
Superimposed complex of unliganded initial structure and final simulated structure of 1B3O

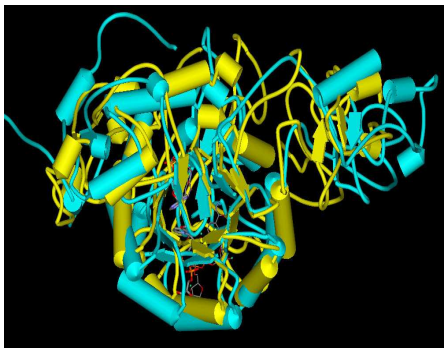

Figure 8
Superimposed complex of ligand bound initial structure and its final simulated structure.

Table 5
Secondary conformation of liganded and unliganded MD-simulated structures.

MD-simulated structures (ns)		Secondary structures		
		α Helix	B Sheet	Coils
Unliganded	1	3-6, 417-421	407-413, 443- 448	1-2, 7-9, 129-139, 159-177, 400-406, 414-416, 422-442, 499-514
	10	417-420	407-413, 443-448	1-9,129-139,159-177,400, 406, 414-416, 421-442, 499-514
	20	418-419, 502-506	401-403, 406-413, 443-448	1-9,129-139,159-177,400,404-405, 414-417,420-442, 499-501,507-514
	30	3-6, 76-84, 97-108, 149-152, 197-203, 256-266, 281-284, 288-292, 307-315, 343-357, 375-377, 418-420, 458-462, 469-470, 499-503	34-38, 53-55, 59-61, 64-66, 89-91, 124-126, 172-174, 209-213, 217-222, 247-250, 270-274, 298-302, 321-323, 321-323360-365, 383-386, 383-386, 401-403, 406-408, 411-413, 443-445, 489-493	7-33, 39-52, 56-58, 67-75, 85-88, 92-96, 109-123, 127-148, 153-171, 175-196, 204-208, 214-216, 223-246, 251-255, 267-269, 275-280, 285-287, 293-297, 303-306, 316-320, 324-342, 366-374, 378-382, 387-400, 404-405, 409-410, 414-417, 421-442, 446-457, 463-468, 471-488, 494-498, 504-514
	40	76-85, 97-108, 197-204, 256-266, 281-284, 288-290, 307-316, 343-355, 374-378, 458-462, 499-503	34-38, 53-55, 59-61, 64-66, 89-91, 124-126, 172-174, 209-213, 217-222, 237-239, 243-245, 247-250, 269-274, 298-302, 320-323, 362-365, 383-386, 407-413, 443-449, 489-493	1-33, 39-52, 56-58, 67-75, 92-96, 109-123, 127-151, 153-171, 175-195, 205-208, 214-216, 223-236, 240-242, 251-255, 275-280, 285-287, 291-297, 303-306, 317-319, 324-342, 356-361-366-373, 379-382, 388-390, 392-406, 414-417, 420-442, 450-457, 463-488, 494-498, 504-514
	50	20-25, 76-84, 97-108, 148-152, 197-204, 256-266, 281-284, 288-290, 307-316, 343-356, 375-378, 387-390, 418-419, 458-464, 499-503	34-38, 53-55, 59-61, 64-66, 89-91, 124-126, 172-174, 209-213, 217-222, 237-239, 243-245, 247-250, 271-274, 298-300, 321-323, 360-365, 383-386, 407-414, 442-449, 489-493	1-19, 26-33, 39-52, 56-58, 67-75, 85-88, 92-96, 109-123, 127-147, 153-171, 175-196, 205-208, 214-216, 223-236, 240-242, 251-255, 267-270, 275-280, 285-287, 291-297, 301-306, 317-320, 324-342, 357-359, 366-374, 379-374, 391-406, 415-417, 420-441, 450-457, 465-488, 494-498, 504-514

Liganded	1	5-8, 20-22, 78-85, 97-109, 176-178, 199-204, 258-265, 281-293, 312-315, 333-336, 343-355, 373-378, 388-390, 453-466, 476-479, 497-501	36-38, 53-55, 64-67, 88-90, 113-115, 221-223, 246-248, 269-273, 298-300, 321-323, 360-364, 383-386, 401-403, 406-415, 441-449, 489-491	1-4, 9-19, 23-35, 39-52, 56-58, 62-63, 68-77, 86-87, 91-96, 110-112, 116-175, 179-198, 205-220, 224-245, 249-257, 266-268, 274-280, 294-297, 301-307, 309-311, 316-320, 324-332, 337-342, 356-359, 365-372, 379-382, 391-400, 416-440, 450-452, 467-475, 480-488, 492-496, 502-514
	10	2-6, 20-23, 78-85, 97-108, 200-204, 254-265, 281-293, 307-316, 334-335, 343-357, 374-378, 388-391, 453-465, 469-471, 476-482, 496-501,	36-38, 53-55, 59-61, 64-68, 128-130, 137-139, 209-211, 220-222, 248-250, 269-273, 298-300, 321-323, 330-332, 360-365, 383-386, 407-415, 441-449, 489-491,	7-19, 24-35, 39-52, 56-58, 69-77, 86-96, 109-127, 131-136, 140-199, 205-208, 212-219, 223-247, 251-253, 274-280, 294297, 301-306, 317-320, 324-329, 336-342, 366-373, 379-382, 392-406, 416-440, 450-452, 466-468, 472-475, 483-488, 492-495, 502-514
	20	2-7, 78-85, 97-108, 176-178, 197-204, 254-266, 281-293, 308-316, 333-337, 344-357, 373-378, 453-465, 476-484	36-38, 53-55, 59-61, 64-70, 72-74, 88-90, 209-211, 220-223, 237-239, 243-245, 248-250, 270-273, 298-300, 321-323, 362-365, 383-386414-416, 418-420, 441-449	8-35, 39-52, 56-58, 62-63, 75-77, 91-96, 109-175, 179-196, 205-208, 212-219, 224-236, 240-242, 251-253, 267-269, 274-280, 294-297, 301-307, 317-320, 324-332, 338-343, 358-361, 366-372, 379-382, 391-406, 421-440, 450-452, 466-468, 485-488,492-514
	30	2-7, 21-23, 78-85, 97-107, 197-204, 254-266, 281-293, 308-316, 333-336, 343-355, 374-378, 388-391, 453-465, 469-471, 476-483, 497-501	53-55, 59-61, 64-70, 72-74, 113-115, 209-211, 220-223, 237-239, 243-245, 247-250, 269-273, 298-300, 321-323, 407-415, 441-449	8-20, 24-52,56-58, 75-77, 86-88, 92-96, 108-112, 116-196, 205-208, 212-219, 224-236, 240-242, 251-253, 274-280, 294-297, 301-307, 317-320, 324-332, 337-342, 356-361, 366-373, 379-382, 392-406, 416-440, 450-452, 466-468, 472-475, 484-496, 502-514
	40	2-5, 21-23, 78-85, 97-108, 176-178, 197-204, 254-265, 282-293, 307-316, 334-336, 343-355, 371-379, 388-390, 453-465, 477-484, 498-499	36-38, 53-55, 59-61, 64-70, 72-74, 209-211, 220-223, 237-239, 243-245, 248-250, 269-273, 298-300, 321-323, 330-332, 360-365, 383-386, 401-403, 406-415, 441-449, 489-491	6-20, 24-35, 39-52, 56-58, 75-77, 86-96, 109-112, 116-175, 179-196, 205-208, 212-219, 224-236, 240-242, 241-253, 266-268, 274-281, 294-297, 301-306, 317-320, 324-329, 337-342, 356-359, 366-370, 380-382, 391-400, 416-440, 450-452, 466-476, 485-488, 492-497, 500-514
	50	2-5, 21-24, 76-85, 97-108, 197-204, 255-266, 281-293, 307-316, 334-335, 343-355, 371-378, 388-390, 453-465, 469-471, 476-484, 497-501	36-38, 53-55, 59-61, 64-70, 72-74, 209-211, 220-222, 237-239, 243-245, 269-273, 298-300, 321-323, 360-365, 383-386, 407-415, 441-449, 489-491	7-20, 25-35, 39-52, 56-58, 86-96, 109-196, 205-208, 212-219, 223-236, 240-242, 246-254, 274-280, 294-297, 301-306, 317-320, 324-333, 336-342, 356-359, 366-370, 379-382, 391-406, 416-440, 450-452, 466-468, 472-475, 485-488, 492-496, 502-514

CONCLUSION

The present study demonstrates the utility of MD-simulation in refining and modeling the static protein structure. The modeled structure of hIMPDH-II may be used as a new attractive target for designing and development of leukemic drug. Conformational transition of the unliganded hIMPDH-II structure (during dynamics) could be helpful for elucidating the details of inter atomic interaction, stability and dynamic character of catalytic / cofactor – binding residues. Modeling of catalytic (IMP and NAD^+ binding pocket) and CBS domains, may shade some light on the functional anatomy of IMPDH enzyme. The computational work could provide a new insight on structural biochemistry of IMPDH.

ACKNOWLEDGEMENTS

B.P.M. acknowledge and is thankful to the Department of Biotechnology (DBT), Govt. of India for providing the research project (BT/PR11696/BID/07/282/2008) and full financial assistance in this work. D.K.M is also thankful to DBT for giving Fellowship to work in this project.

REFERENCES

1. McLean JE, Hamaguchi N, Helenky P, Mourtimer ES, Stanton M and Hedstrom L, Inosine 5'-monophosphate dehydrogenase binds nucleic acids in vitro and in vivo, Biochem. J., 379: 243-51, (2004).
2. Prosise GL and Luecke H, Crystal structures of Tritrichomonasfoetus inosine monophosphate dehydrogenase in complex with substrate, cofactor and analogs: a structural basis for the random-in ordered-out kinetic mechanism, J. Mol. Biol., 326: 517–527, (2003).
3. Hedstrom L, IMP dehydrogenase: structure, mechanism, and inhibition, Chem. Rev., 109: 2903–2928, (2009).
4. Bairagya HR, Mukhopadhyay BP and Bera AK, Role of Salt bridge Dynamics in inter domain recognition of Human IMPDH Isoforms: An Insight to inhibitor Topology for isoform –II, J. Biomol. Struct. Dyn., 29: 441-462, (2011).
5. Bairagya HR, Mukhopadhyay BP, Malik P and Srivastava AK, Conserved Water Mediated H-bonding Dynamics of Carboxamide group in NAD to Catalytic Asp 274 and His 93 in Human IMPDH, J. Biomol. Struct. Dyn., 28: 1008-1010, (2011).
6. Bairagya HR and Mukhopadhyay BP, Conserved water mediated inter-domain recognition in IMPDH-II (human), J. Bimolecular Structure & Dynamics, 26: 855, (2009).
7. Risal D, Stricker MD and Goldstein BM, Crystal structure of human type II inosine monophosphate dehydrogenase: implications for ligand binding and drug design, Proc. Natl. Acad. Sci., 96: 3531-3536, (1999).
8. Risal D, Stricker MD and Goldstein BM, Structure Deposite RCSB, (2004).
9. Risal D, Stricker MD and Goldstein BM, Structure Deposite, RCSB (2004).
10. Colby TD, Vanderveen K, Strickler MD, Markham GD and Goldstein BM, Crystal structure of human type II inosine monophosphate dehydrogenase: Implications for ligand binding and drug design, Proc. Natl. Acad. Sci., 96: 3531–3536, (1999).
11. Bairagya HR, Mukhopadhyay BP and Bera AK, Conserved water mediated recognition and the dynamics of active site Cys 331 and Tyr 411 in hydrated structure of human IMPDH-II, J. Mol. Recognit., 24: 35–44, (2011).
12. Berman HM, Bhat TN, Bourne PE, Gilliand G, Feng Z, Shindyalov IN, Westbrook J and Weissig H, Announcing the worldwide

protein data bank, Nat. Struct. Biol., 10: 980, (2003).
13. Guex N and Peitsch MC, SWISS-MODEL and the Swiss-PdbViewer: an environment for comparative protein modelling, Electrophoresis, 18: 2714–2723, (1997).
14. Guex N, Diemand A, Peitsch MC and Schwede T, Glaxo Smith Kline R.D., (2001).
15. Gunsteren VWF and Berendsen HJC, Computer Simulation of Molecular Dynamics: Methodology, Applications and Perspectives in Chemistry, Chem. Int. Ed. Engl., 29: 992–1023, (1990).
16. Pisabarro MT, Ortiz AR, Serrano L and Wade RC, Homology Modeling of the Abl-SH3 domain, Proteins, 20: 203–215, (1994).
17. Levitt M and Sharon R, Accurate Simulation of Protein Dynamics in Solution, Proc. Natl. Acad. Sci., 85: 7557-7561, (1998).
18. Yokomizo T, Nakasako M, Yamazaki T, Shindo H and Higo J, Hydrogen-bond patterns in the hydration structure of a protein, Chemical Physics letters, 48: 332-336, (2005).
19. Bairagya HR, Mukhopadhyay BP and Bhattacharya S, Role of the conserved water molecules in the binding of inhibitor to IMPDH-II (human): A study on the water mimic inhibitor design. J. Mol. Struct. Theochem., 908: 31–39, (2009).
20. Bairagya HR, Mukhopadhyay BP and Sekar K, Conserved Water Mediated Inter-Domain Recognition in IMPDH-II (human), J. Biomol. Struct. Dyn., 26: 497-508, (2009).
21. Bairagya HR, Mukhopadhyay BP and Sekar K, An Insight to the Dynamics of Conserved Water Molecular Triad in IMPDH II (Human): Recognition of Cofactor and Substrate to Catalytic Arg 322. J. Biomol. Struct. Dyn. 27: 149–158, (2009).
22. Fleming PJ, Fitzkee MM, George DR, Mezei M, Nicholas C and Rajgopal S, A novel method reveals that solvent water favors polyproline II over β-strand conformation in peptides and unfolded proteins: conditional hydrophobic accessible surface area (CHASA), Protein Sci. 14: 111–118, (2005).
23. MacKerell AD, Bellott M, Dunbrack RL, Fischer MJ, Guo S, Ha JH, Joseph S, Jr Bashford D, Jr Evanseck RL, Field J, Kuchnir D, Kuczera L, Karplus MD, Lau K, Mattos FTK, Michnick C, Ngo S, Nguyen T, Prodhom DT, Reiher B, Roux IWE, Schlenkrich B, Smith M, Stote J, Straub R,Watanabe J, Kuczera M and Yin J, All-atom empirical potential for molecular modeling and dynamics Studies of proteins, J. Phys. Chem., 102: 3586–3616, (1998).
24. Brooks BR, Bruccoleri RE, Karplus M, Olafson BD, States DJ and Swaminathan S, CHARMM: A program for macromolecular energy, minimization, and dynamics calculations, J. Comput. Chem., 4: 187–217, (1983).
25. Humphrey W, Dalke A and Schulten K, VMD - Visual Molecular Dynamics, J. Mol. Graph, 14: 33–38, (1996).
26. Grayson P, Schulten K and Tajkhorshid E, Mechanisms of selectivity in channels and enzymes studied with interactive molecular dynamics, Biophys. J., 85: 36–48, (2003).
27. Kale L, Bhandarkar M, Brunner R, Gursoy A, Krawetz N, Phillips J, Skeel R, Shinozaki A, Schulten K and Varadarajan K, NAMD2: Greater scalability for parallel molecular dynamics, J. Comp. Phys., 151: 283–312, (1999).
28. Phillips JC, Braun R, Wang W, Gumbart J, Tajkhorshid E, Villa E, Chipot C, Skeel RD, Kale L and Schulten K, Scalable molecular dynamics with NAMD, J. Comp. chem., 26: 1781–1802, (2005).
29. Gullingsrud J, Kosztin D and Schulten K, Structural determinants of MscL gating studied by molecular dynamics simulations, Biophys. J., 80: 2074–2081, (2001).
30. Karplus M and Petsko GA, Molecular Dynamics Simulations in Biology, Nature, 347: 631–639, (1990).
31. Bairagya HR, Mukhopadhyay BP and Bhattacharya S, An Insight to the Dynamics of Conserved Water Molecular Triad in IMPDH II (Human): Recognition of Cofactor

and Substrate to Catalytic Arg 322. J. Bio. Mol. Struct. Dyn., 27(2): 149-158, (2009).
32. Laskowski RA, MacArthur MW, Moss DS and Thornton JM, PROCHECK: a program to check the stereochemical quality of protein structures, J. Appl. Crystallogr., 26: 283–291, (1993).
33. Colovos C and Yeates TO, Verification of protein structures: Patterns of nonbonded atomic interactions, Protein Sci., 2: 1511–1519, (1993).
34. Willard L, Ranjan A, Zhang H, Monzavi H, Boyko RF, Sykes BD and Wishart DS, VADAR: a web server for quantitative evaluation of protein structure quality, Nucleic Acids Res., 31: 3316 – 3319, (2003).
35. Lovell SC, Davis IW, Arendall WB, Bakker de PI, Word JM, Prisant MG, Richardson JS and Richardson DC, Structure validation by Calpha geometry: phi,psi and Cbeta deviation, Proteins, 50: 437–450, (2003).
36. Sippl MJ, Recognition of Errors in Three-Dimensional Structures of Proteins, Proteins, 17: 355 – 362, (1993).
37. Weiderstein M and Sippl MJ, ProSA-web: Interactive web service for the recognition of errors in three-dimensional structures of proteins, Nucleic Acid Res., 35: 407-410, (2007).
38. Luthy R, Bowie JU and Eisenberg D, Assessment of protein models with three-dimensional profiles, Nature, 356: 83–85, (1992).
39. Schymkowitz J, Berg F, Stricher F, Rousseau F and Serrano L, The FoldX web server: an online force field, Nucleic Acid Res., 33: 382-388, (2005).
40. 40. Willard L, Ranjan A, Zhang H, Monzavi H, Boyko RF, Sykes BD and Wishart DS, VADAR: A web server for quantitative evaluation of protein structure quality, Nucleic Acids Res., 31(13): 3316-3319, (2003).
41. Šali A and Blundell TL, Comparative protein modelling by satisfaction of spatial restraints. J. Mol. Biol., 234: 779-815, (1993).
42. Zoete V, Cuendet MA, Grosdidier A and Michielin O, J. Comput. Chem, 2011, in press. DOI: 10.1002/jcc.21816.